Electronic Supporting Information

Salicylaldimine functionalized L-phenylalanine-based pseudopeptides: Zinc-instructed conformational tuning of self-assembled nanostructure

Kamlesh Kumar Nigam, Surabhi Asthana and Mrituanjay D. Pandey*

Department of Chemistry, Institute of Science, Banaras Hindu University, Varanasi-221005, India. E-mail: mdpandey.chem@bhu.ac.in

Content:

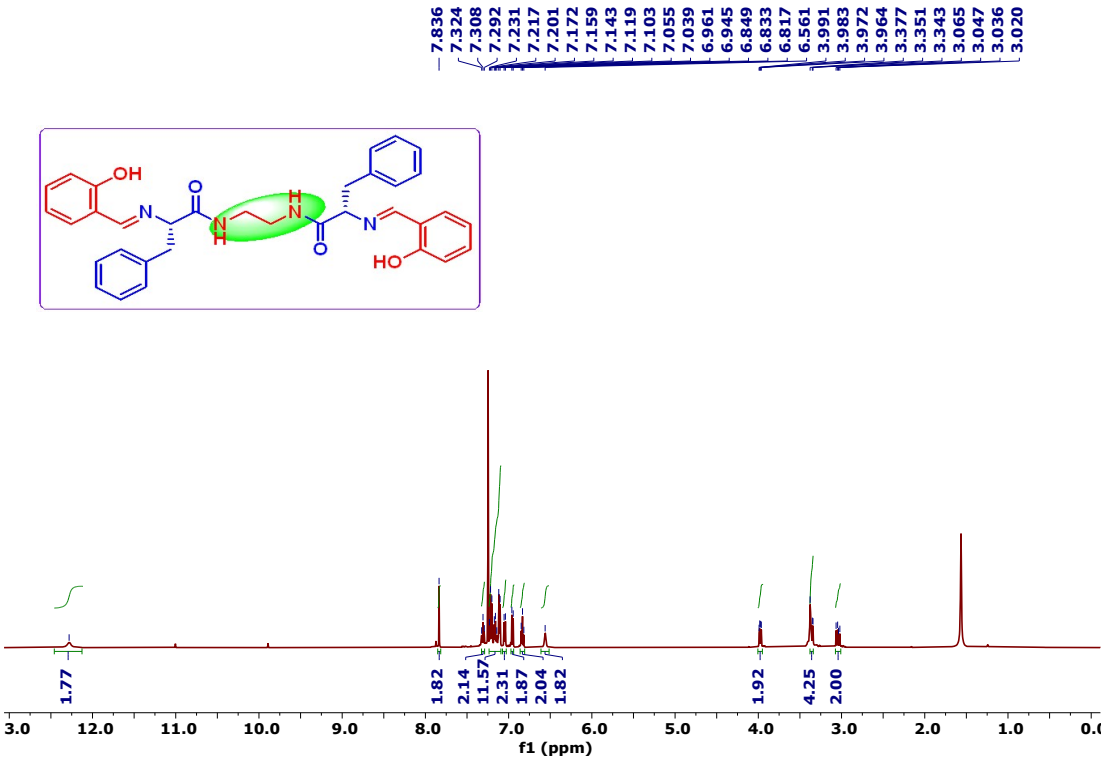

Figure. S1 ^{1}H NMR (500 MHz, $CDCl_3$) **1**

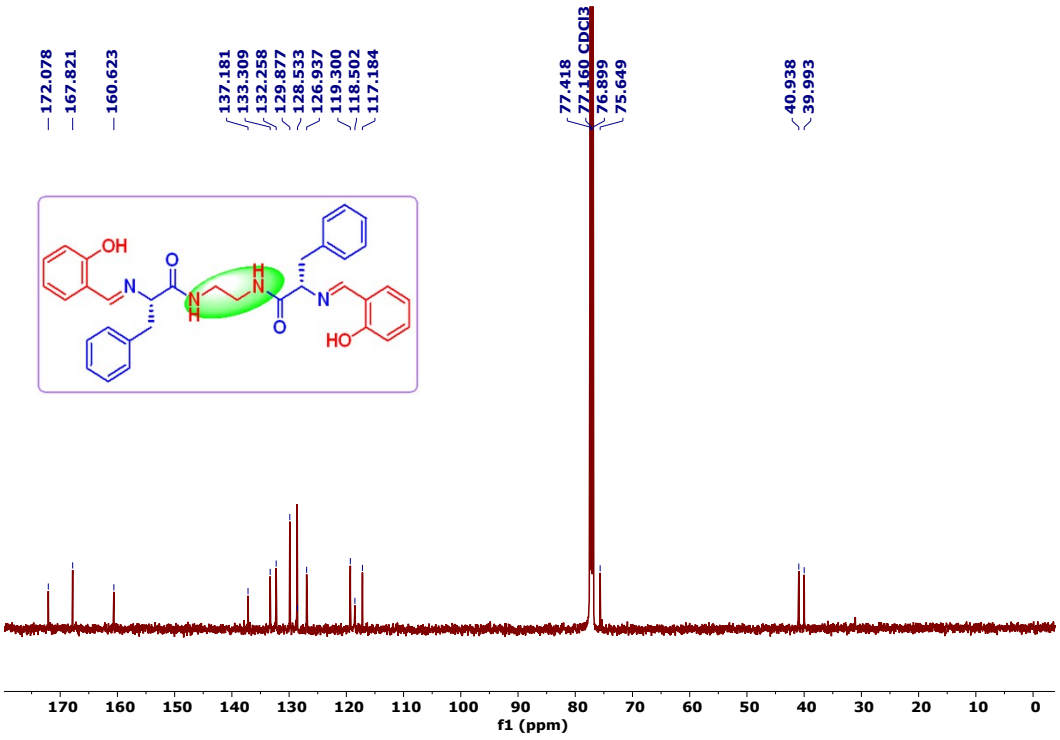

Figure. S2 $^{13}C\{^{1}H\}$ NMR (126 MHz, $CDCl_3$) of **1**

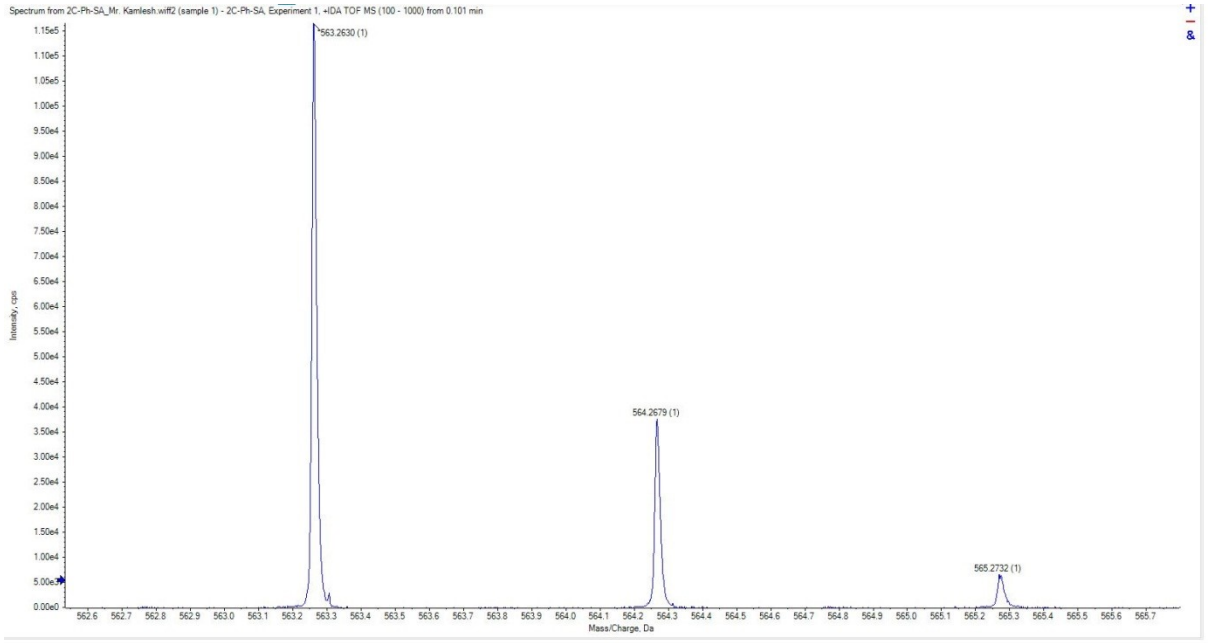

Figure. S3 HRMS data of **1**

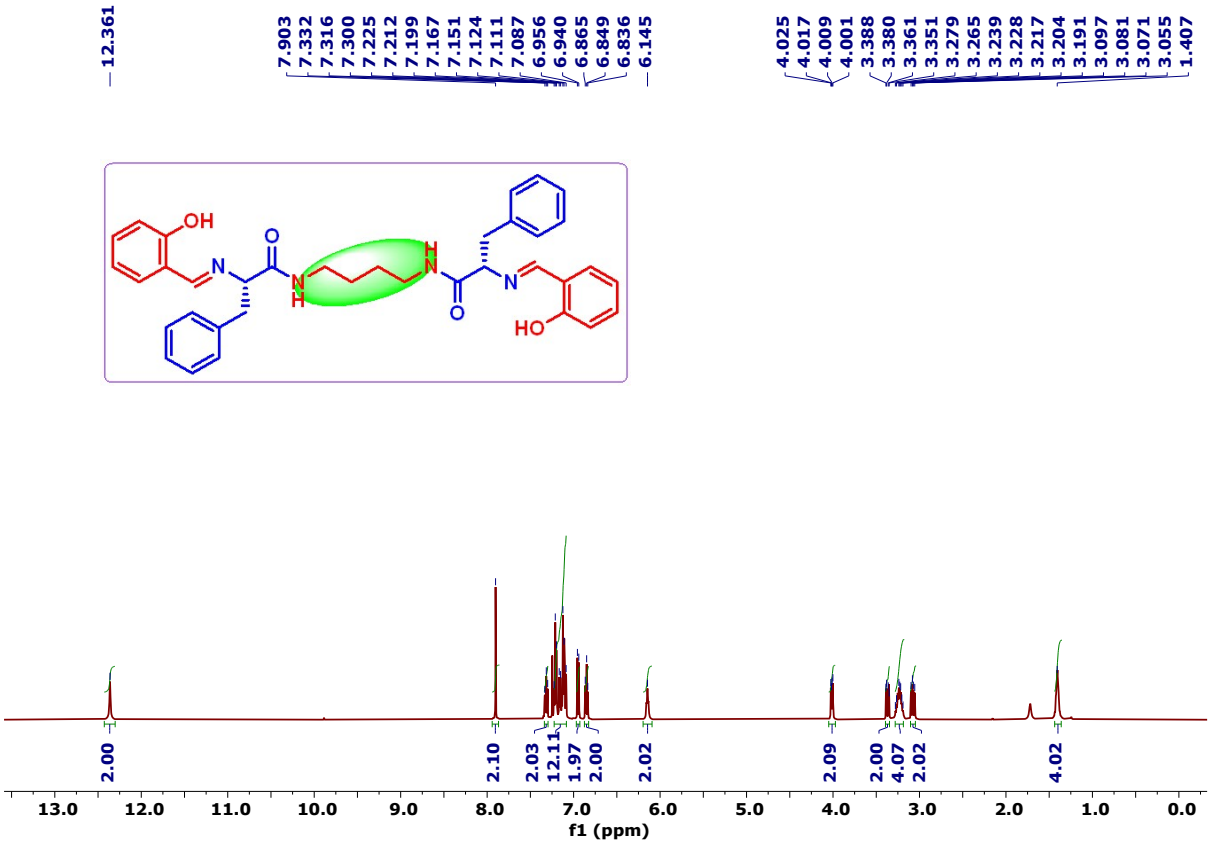

Figure. S4 ^{1}H NMR (500 MHz, $CDCl_3$) of **2**

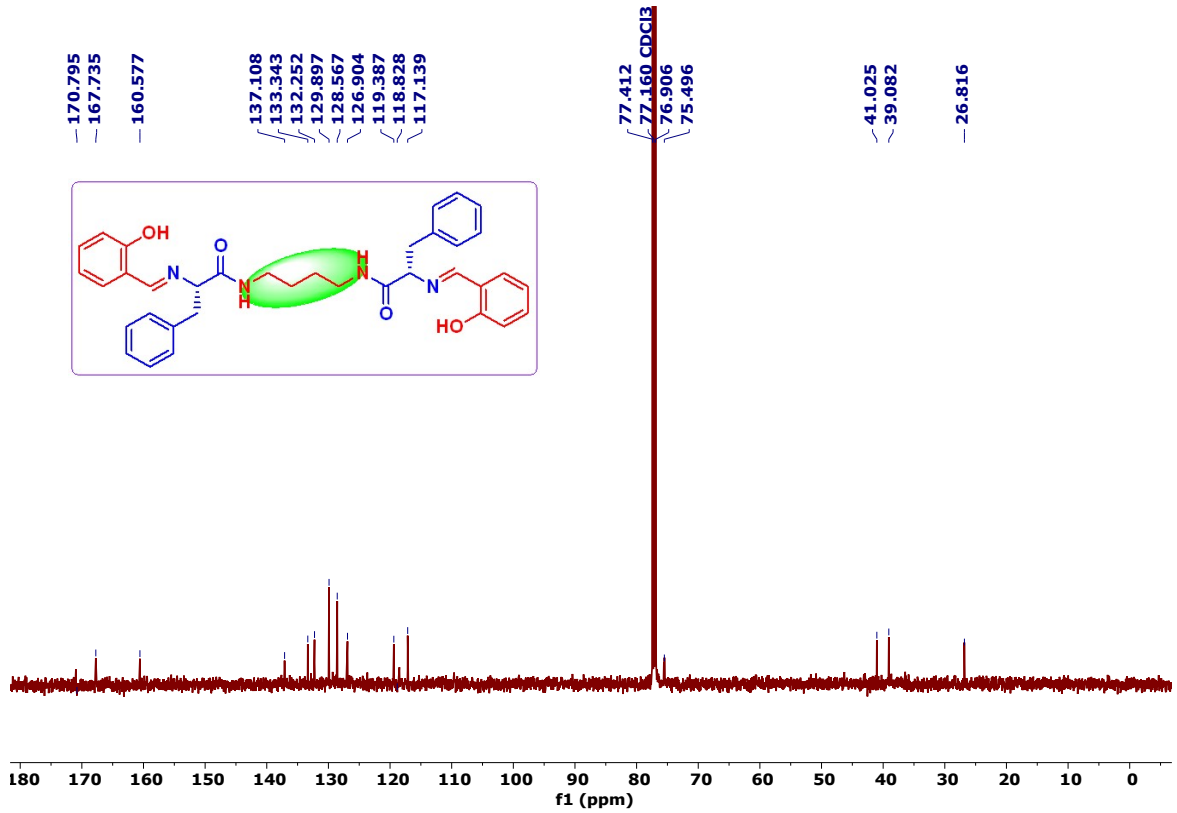

Figure. S5 $^{13}C\{^{1}H\}$ NMR (126 MHz, $CDCl_3$) of **2**

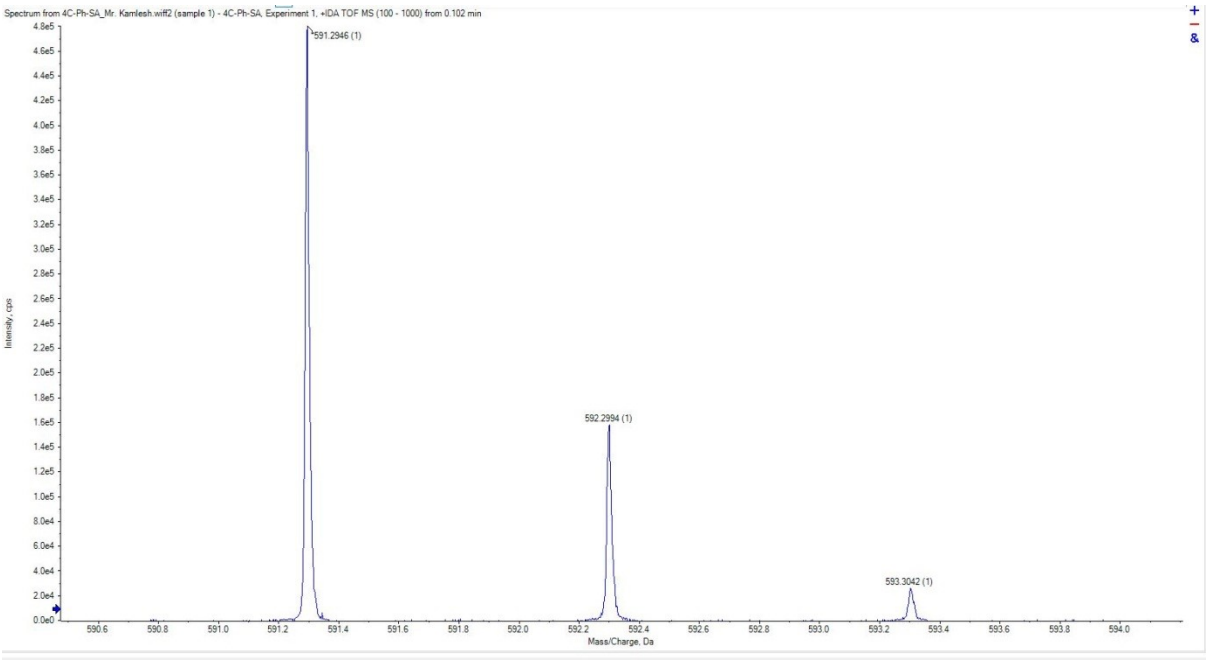

Figure. S6 HRMS data of **2**

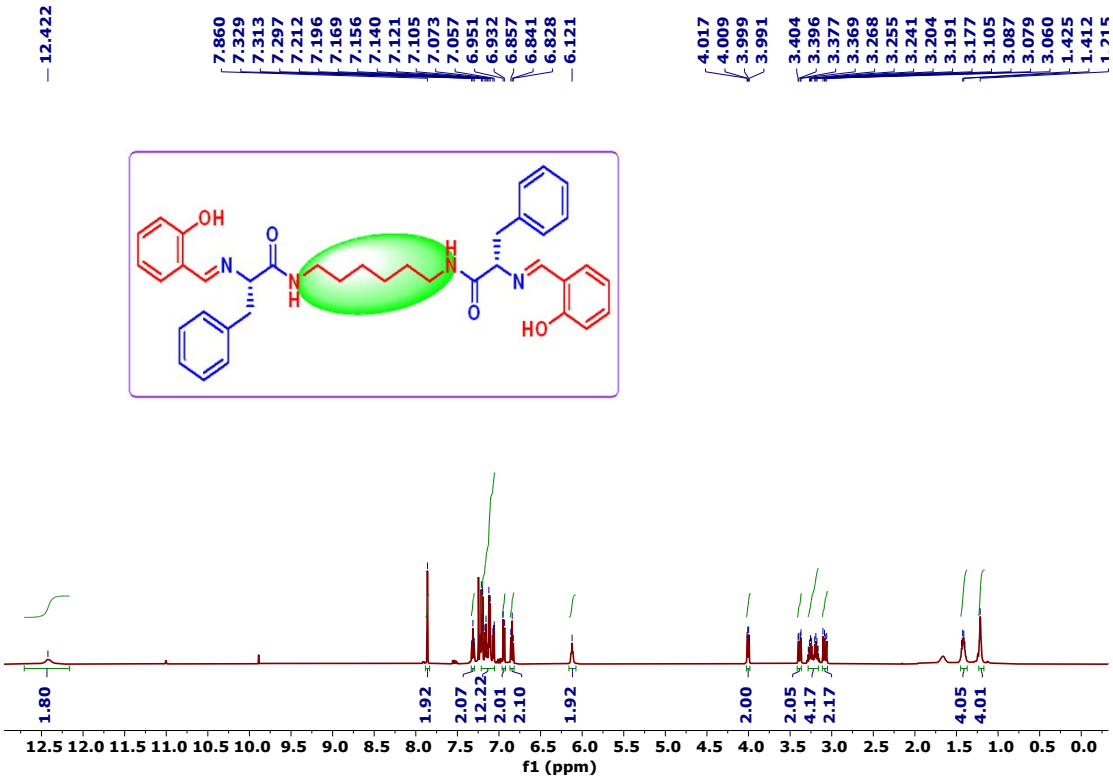

Figure. S7 ^{1}H NMR (500 MHz, $CDCl_3$) of **3**

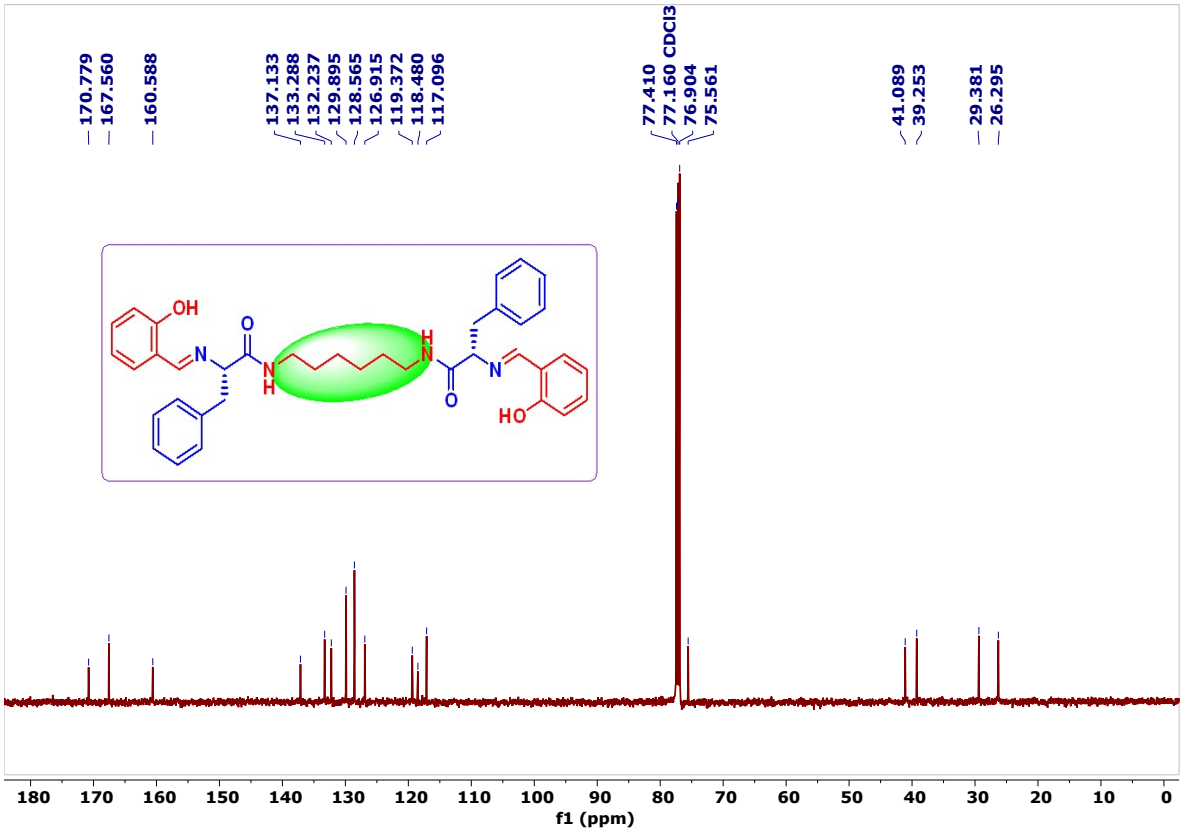

Figure. S8 $^{13}C\{^{1}H\}$ NMR (126 MHz, $CDCl_3$) of **3**

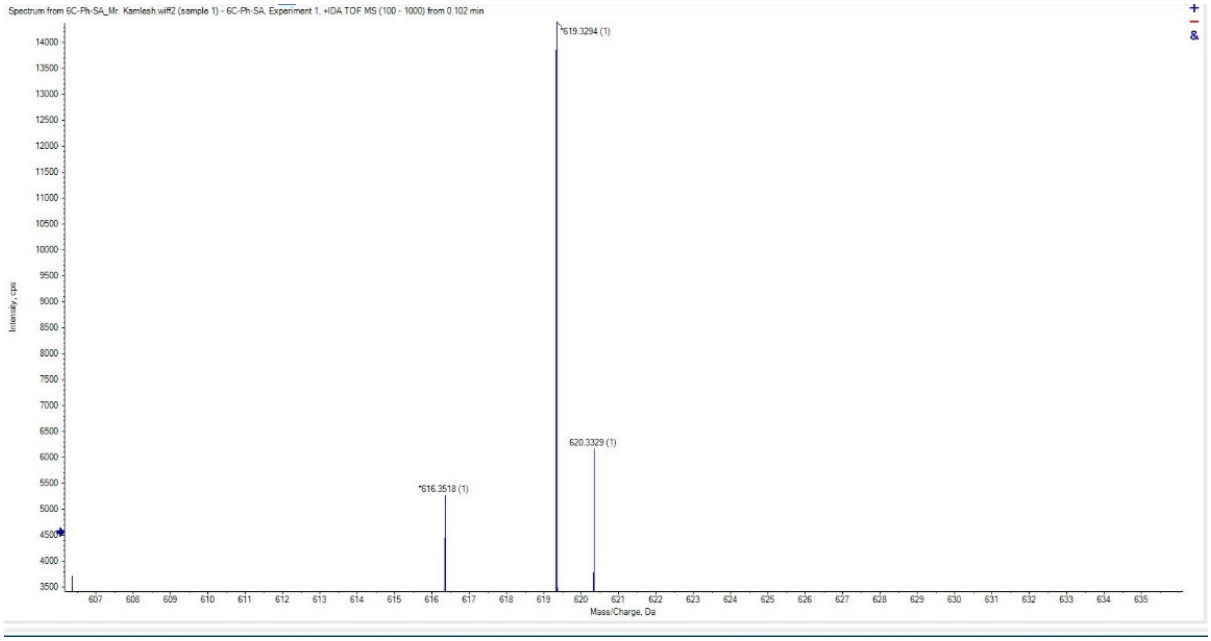

Figure. S9 HRMS data of **3**

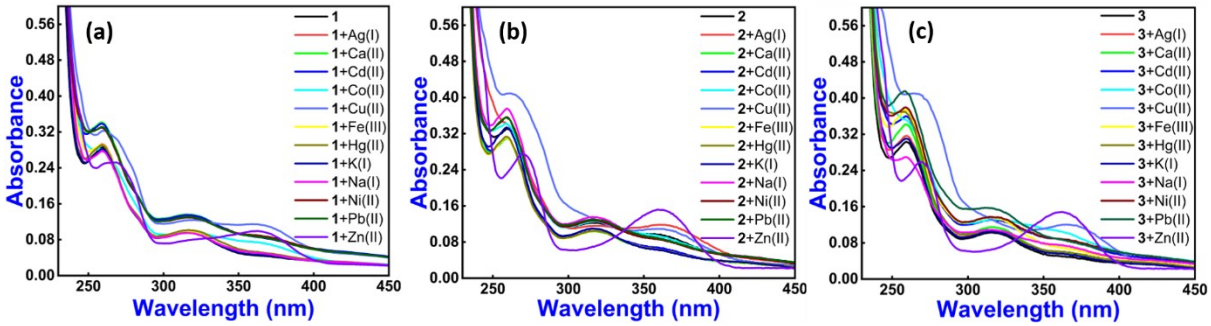

Figure S10 Absorption spectrum of **1** (a), **2** (b) and **3** (c) with various metal ions in HEPES buffer (Ethanol:Water = 3:7 v/v, pH ~ 7.4; 10 μM; at r.t.)

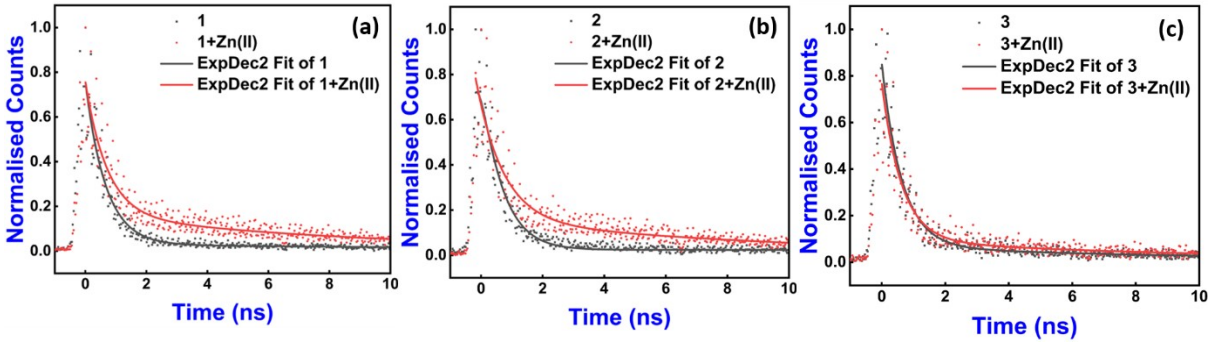

Figure. S11 Fluorescence life time decay curve of **1**(a), **2**(b), and **3**(c) with Zn(II) ions.

Figure. S12 Photographs of **1**(a), **2**(b), and **3**(c) interacting with metal ions under 365 nm UV light illumination.

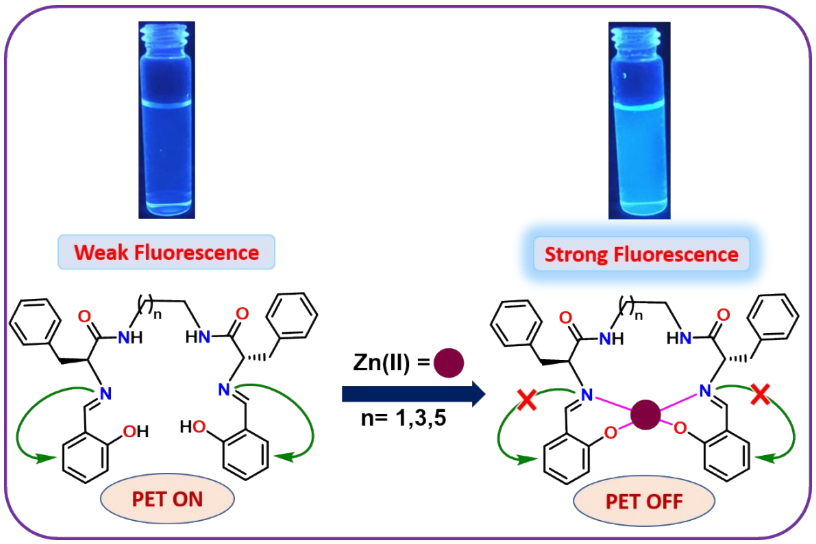

Figure S13. Proposed PET mechanism of **1-3** with Zn(II) ion.

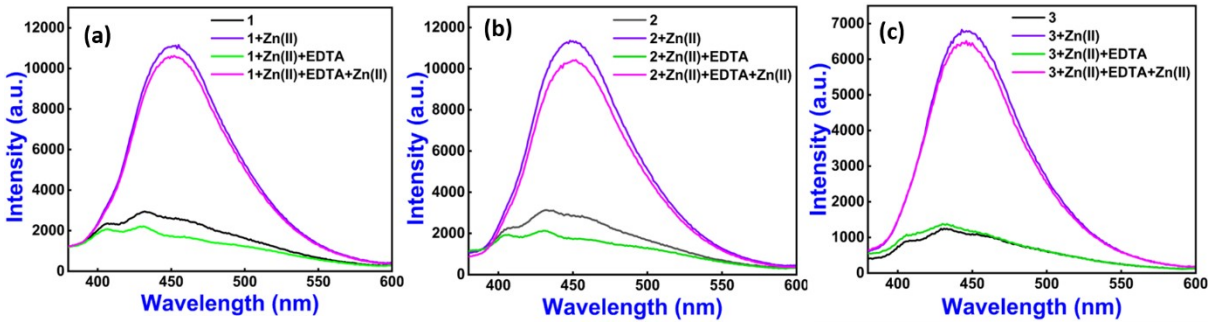

Figure S14. Reversibility study of **1**-Zn(II) (a), **2**-Zn(II) (b), and **3**-Zn(II) (b) complex with EDTA.

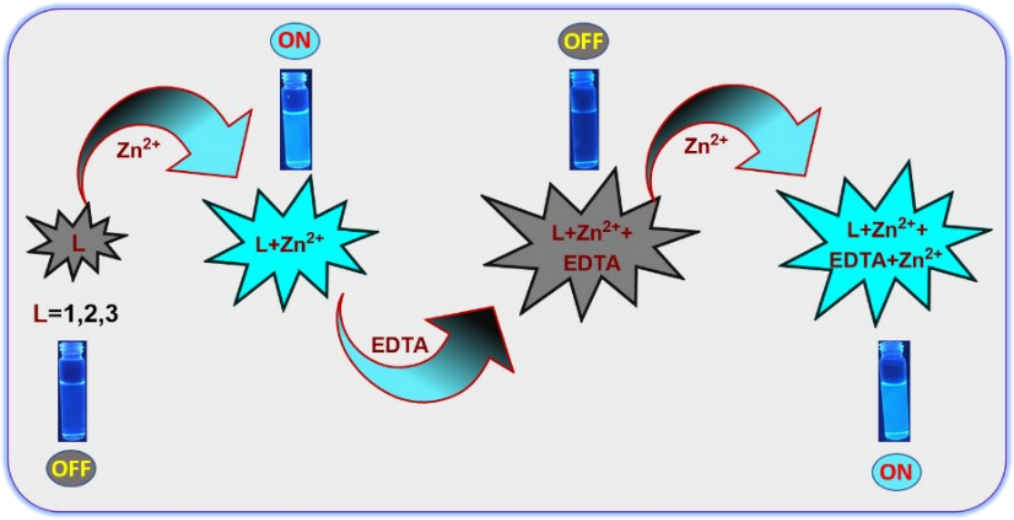

Figure S15. Proposed scheme of reversibility for **1-3**

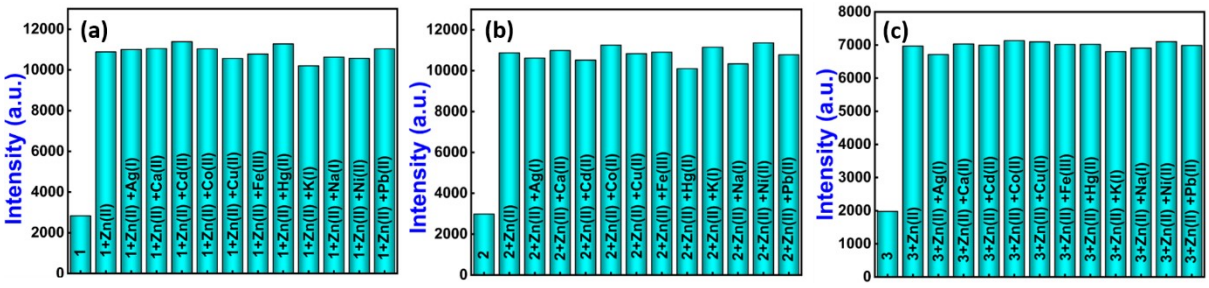

Figure S16. Interference experiments of **1**-Zn(II) (a), **2**-Zn(II) (b), and **3**-Zn(II) (c) complex with other competitive metal ions at room temperature.

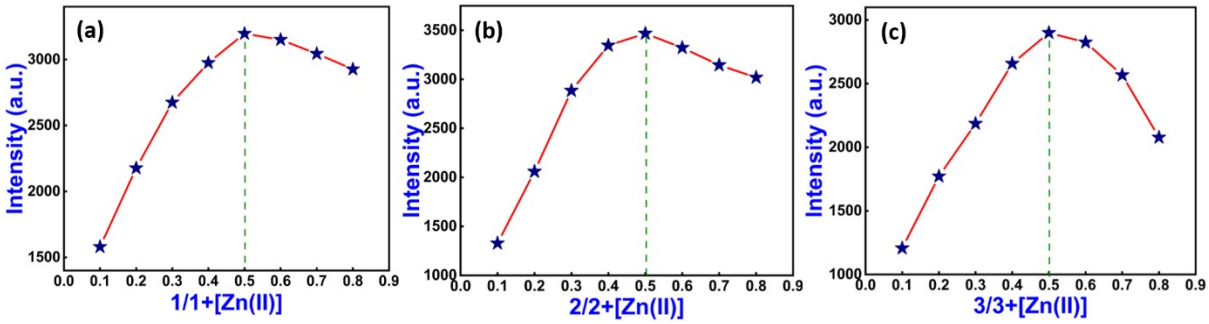

Figure S17. Jobs plot of **1**-Zn(II) (a), **2**-Zn(II) (b), and **3**-Zn(II) (c) complex.

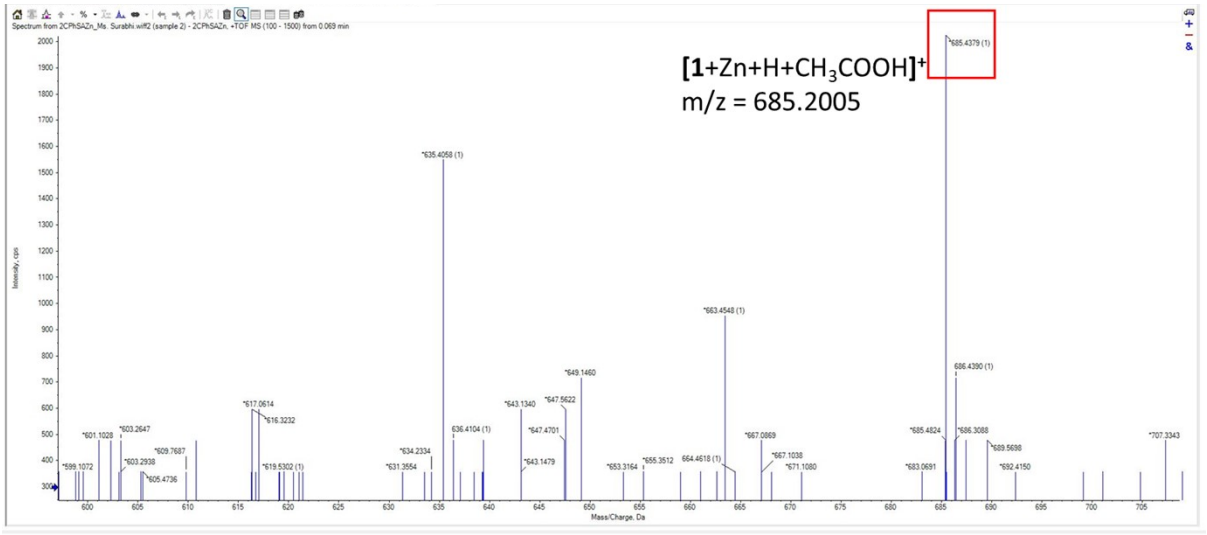

Figure S18. HRMS data of **1**-Zn(II)

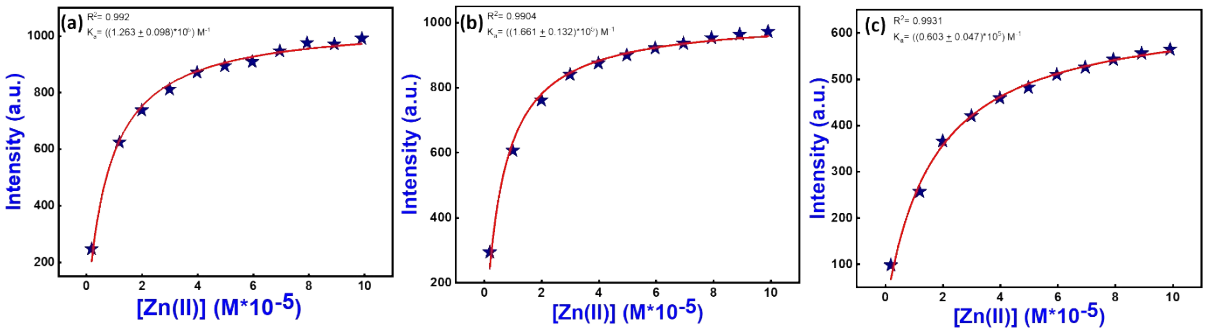

Figure S19. Binding isotherm plots of **1**-Zn(II) (a), **2**-Zn(II) (b), and **3**-Zn(II) (c).

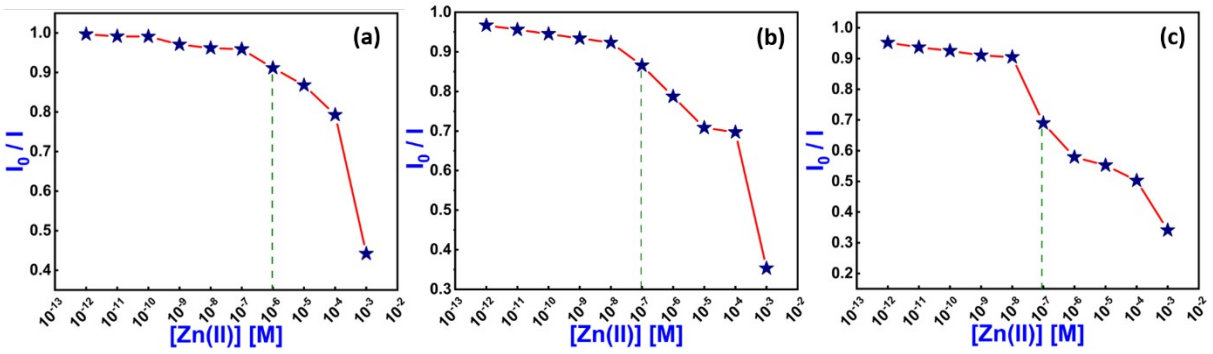

Figure S20. Sensitivity plots of **1**(a), **2**(b), and **3**(b) complex with different concentration of Zn(II) ion (10^{-2} – 10^{-12} M) at room temperature.

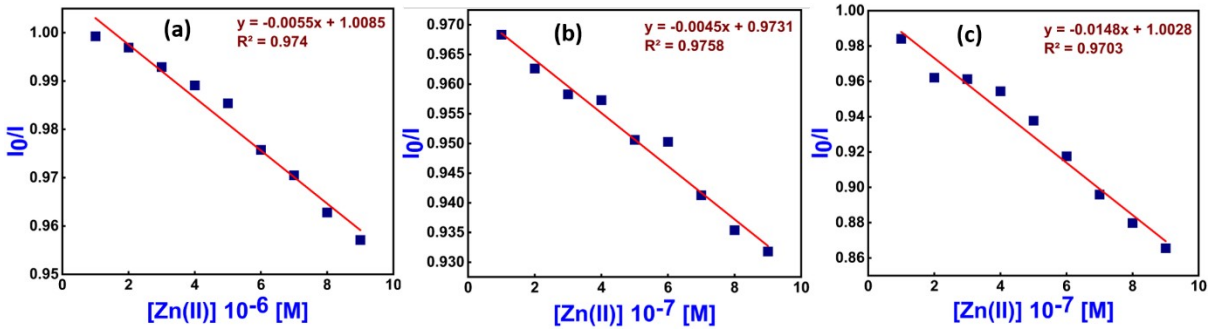

Figure S21. LOD plots of **1**(a), **2**(b), and **3**(b) with different concentrations of Zn(II) ion. (1×10^{-6} M to 9×10^{-6} M for **1** and 1×10^{-7} M to 9×10^{-7} M for both **2** and **3** via; fluorescence spectra).

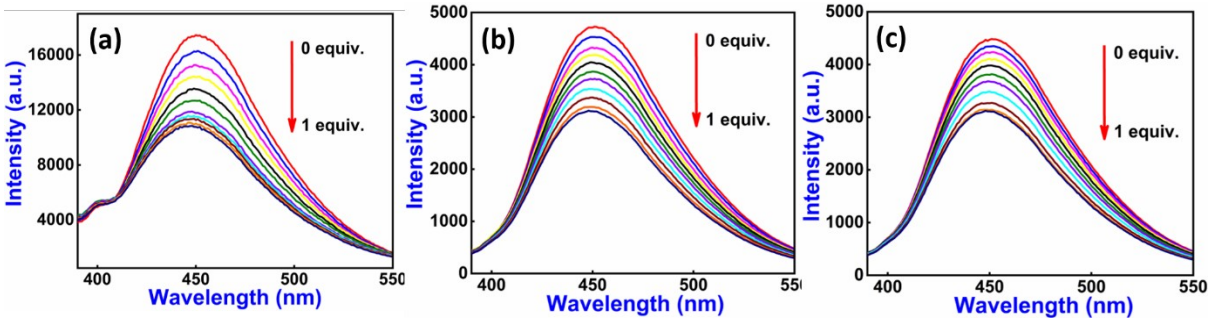

Figure S22. Emission titration spectrum of **1**-Zn(II) (a)**, 2**-Zn(II) (b)**,** and **3**-Zn(II) (c) with BSA (0 to 1 equiv.) in HEPES buffer (Ethanol:Water = 3:7 v/v, pH ~ 7.4; at r.t.)

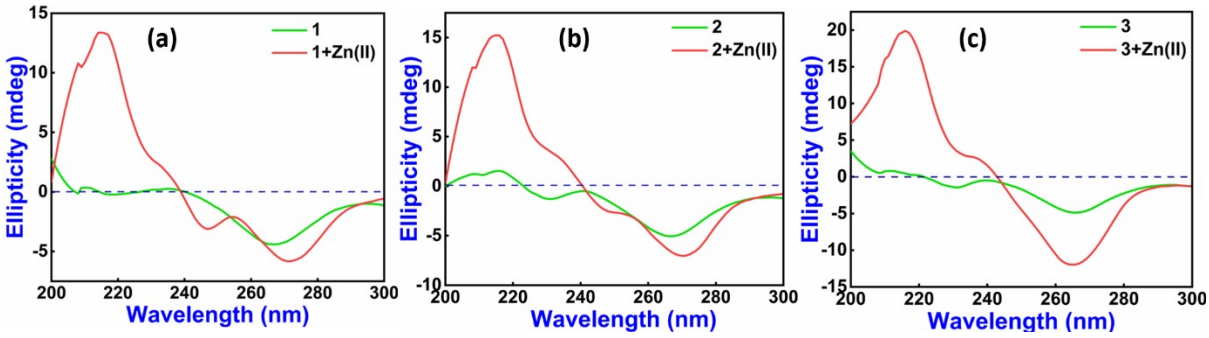

Figure S23. CD spectra of **1**(a), **2**(b), and **3**(b) with Zn(II) ion recorded in Ethanol:Water = 3:7 v/v, 10μM; at r.t.

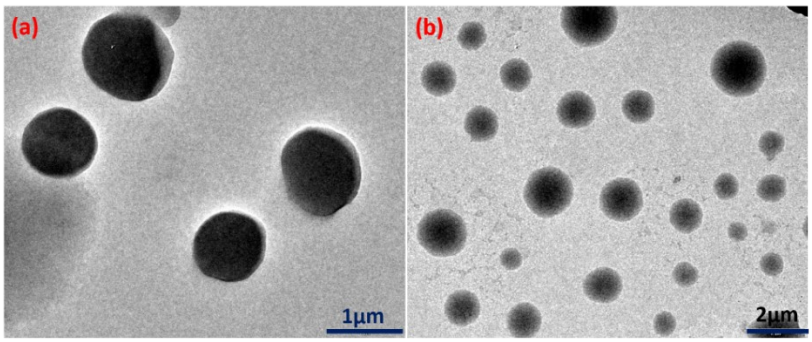

Figure S24. TEM image **1** (a) and **1**-Zn(II) complex (b)

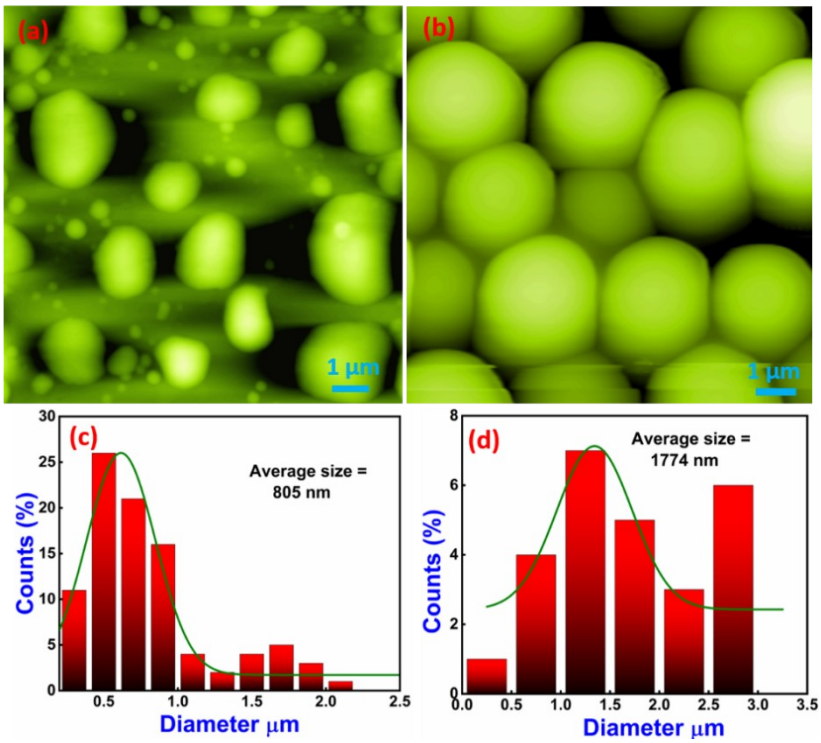

Figure S25. (a) 2D AFM images of self-assembled structure for **2**, (c) its corresponding particle (Spherical) size distribution histogram, (b) 2D AFM images of self-assembled structure for **1**-Zn(II) complex, (d) its corresponding particle (Spherical) size distribution histogram.

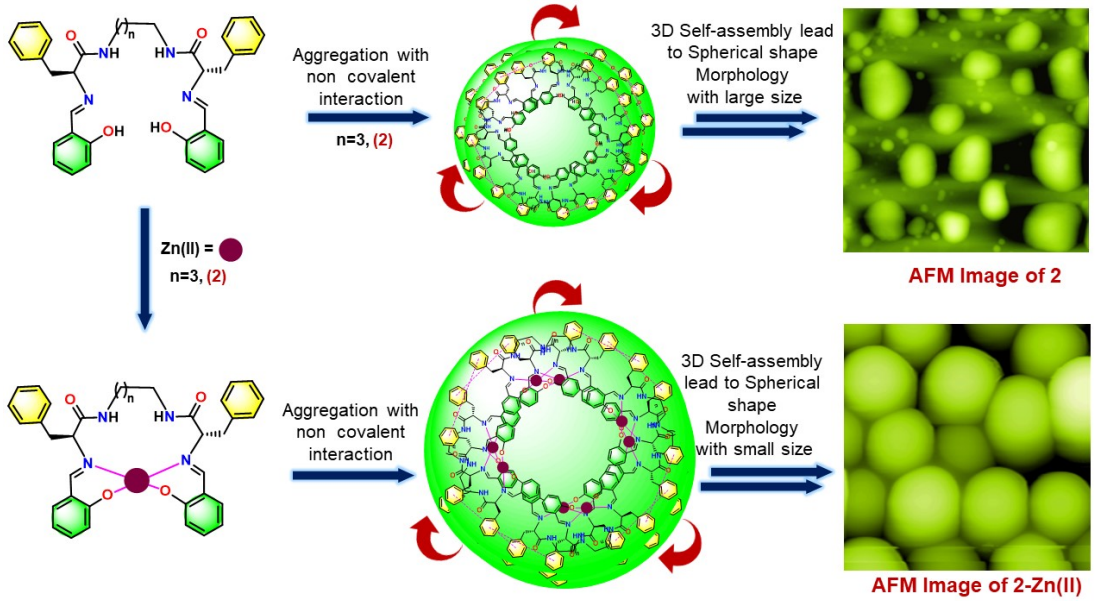

Figure S26. Proposed model to represent the change in structural morphology of **2** by adding Zn(II) ions via 2D AFM image.

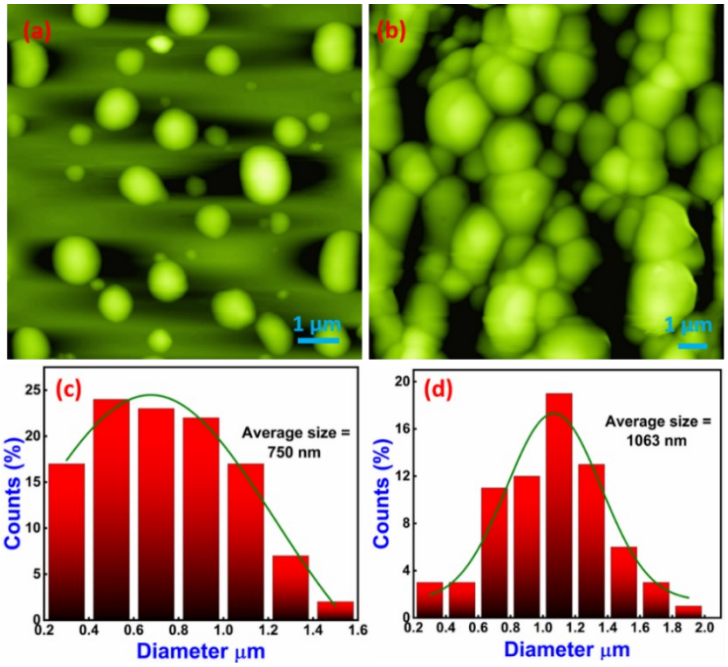

Figure S27. (a) 2D AFM images of self-assembled structure for **3**, (c) its corresponding particle (Spherical) size distribution histogram, (b) 2D AFM images of self-assembled structure for **3**-Zn(II) complex, (d) its corresponding particle (Spherical) size distribution histogram.

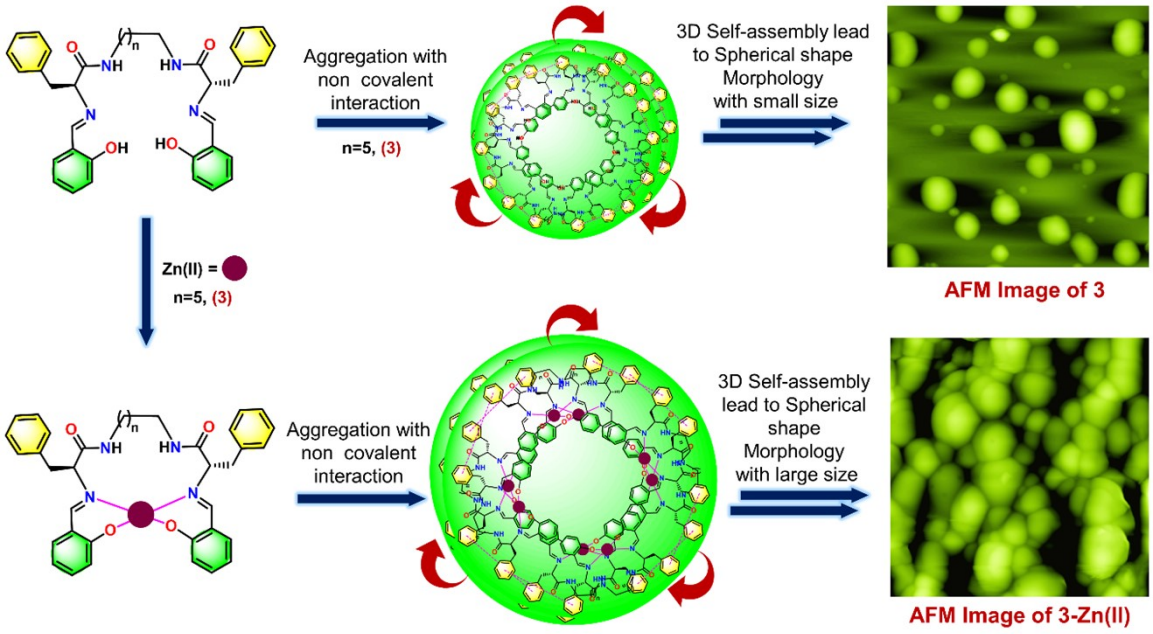

Figure S28. Proposed model to represent the change in structural morphology of **3** by adding Zn(II) ions via 2D AFM image.

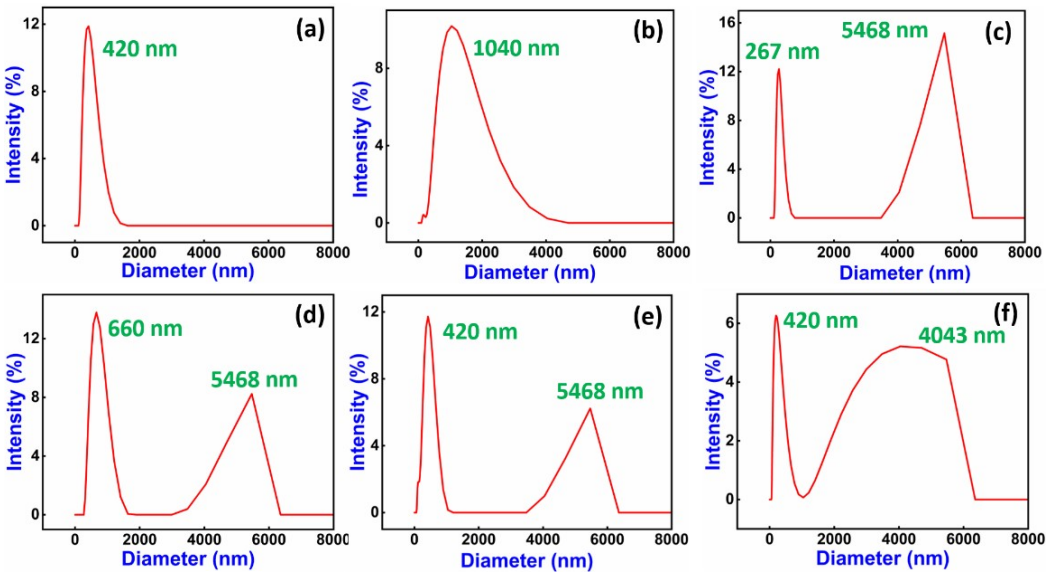

Figure S29. The particle size distribution analyzed through Dynamic Light Scattering (DLS) spectra for compounds **1** (a), **2** (b), **3** (c) and its complex **1**-Zn(II) (d), **2**-Zn(II) (e), **3**-Zn(II) (f) in a solution of Ethanol:Water at a ratio of 3:7 v/v (10μM).

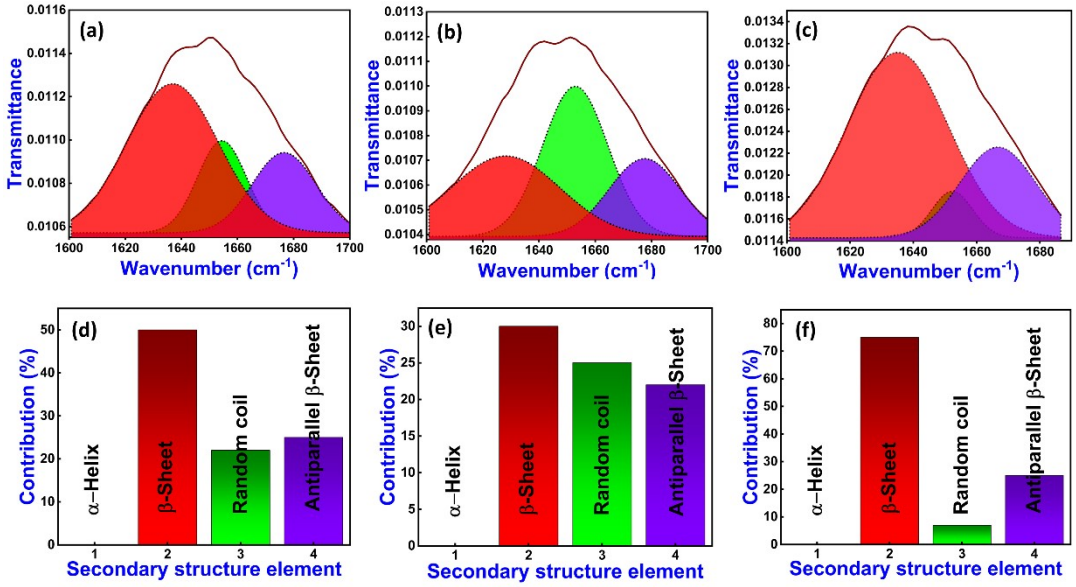

Figure S30. (a) The FT-IR spectrum of **1**-Zn(II) (solid brown line) and its deconvolution (dashed colorful area), (d) Secondary structure contributions of **1**-Zn(II) in self-assembly, (b) The FT-IR spectrum of **2**-Zn(II) (solid brown line) and its deconvolution (dashed colorful area), (e) Secondary structure contributions of **2**-Zn(II) in self-assembly. (c) The FT-IR spectrum of **3**-Zn(II) (solid brown line) and its deconvolution (dashed colorful area), (f) Secondary structure contributions of **3**-Zn(II) in self-assembly. Fitting of deconvolution plot by multiple Gaussian peaks in the amide region ranging from 1600 to 1700 cm^{-1}.

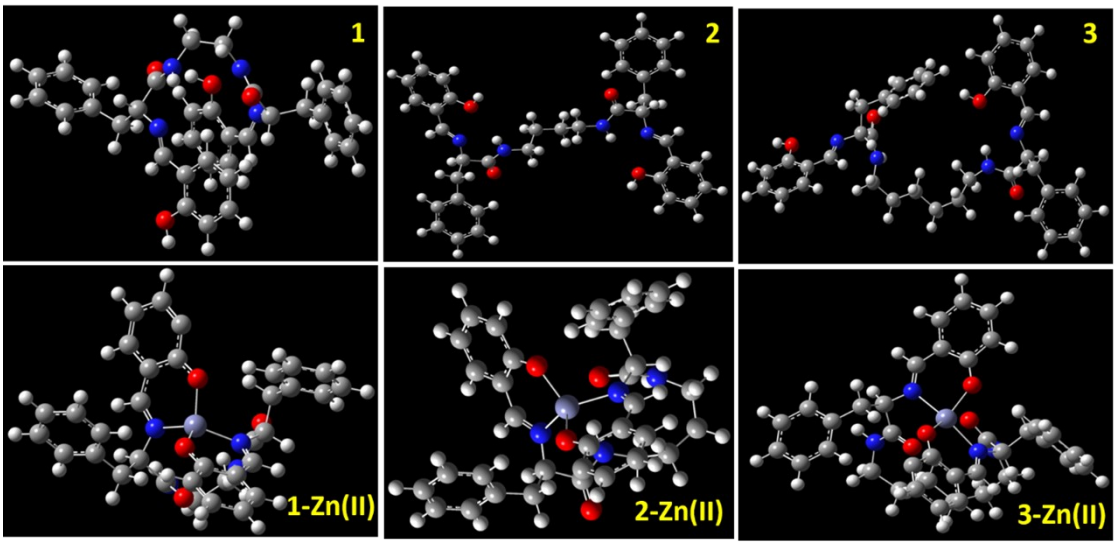

Figure S31. DFT- optimized structure of **1-3** and its complex **1-3**-Zn(II))

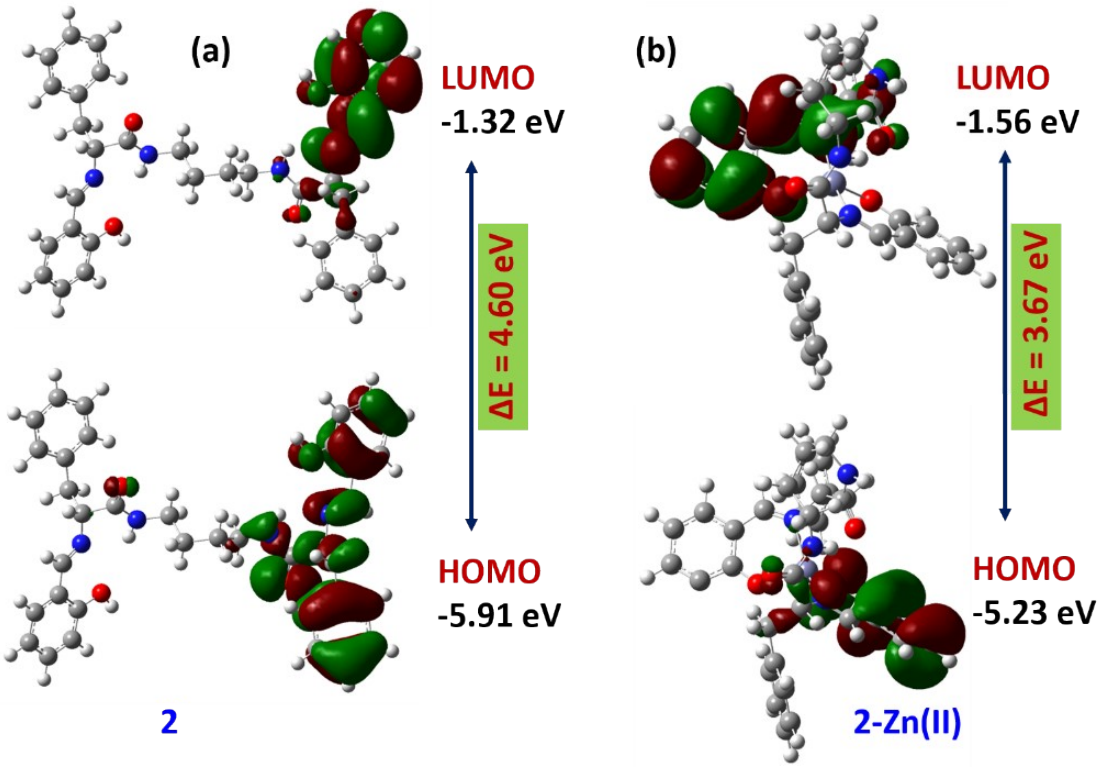

Figure S32. Optimized energy level and energy gap between HOMO-LUMO of **2** (a) and **2**-Zn(II) complex (b)

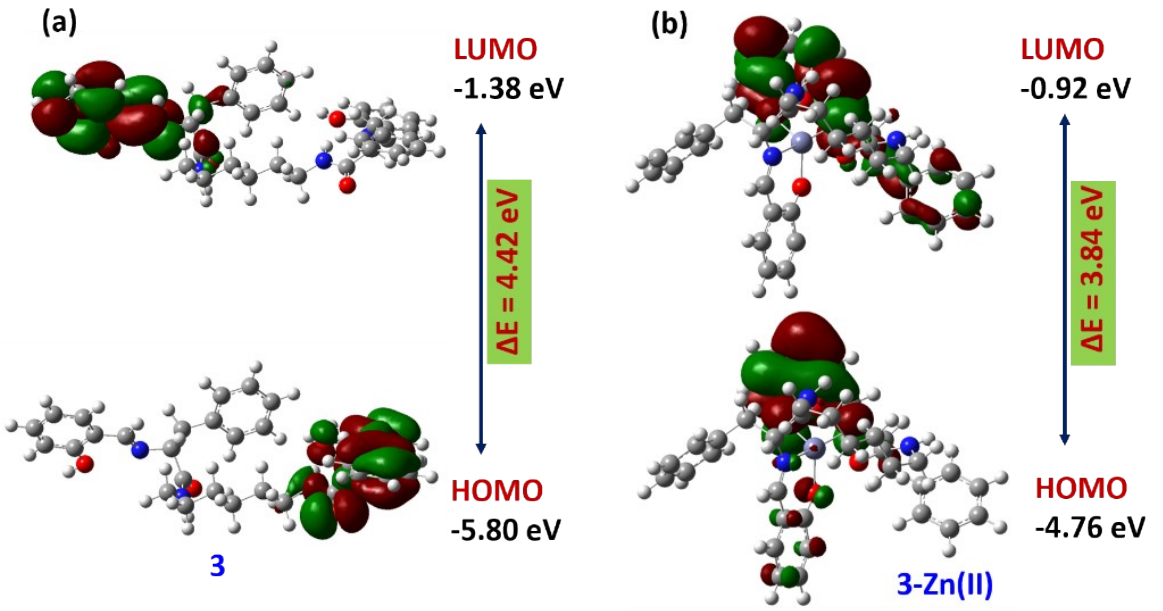

Figure S33. Optimized energy level and energy gap between HOMO-LUMO of **3** (a) and **3**-Zn(II) complex (b).

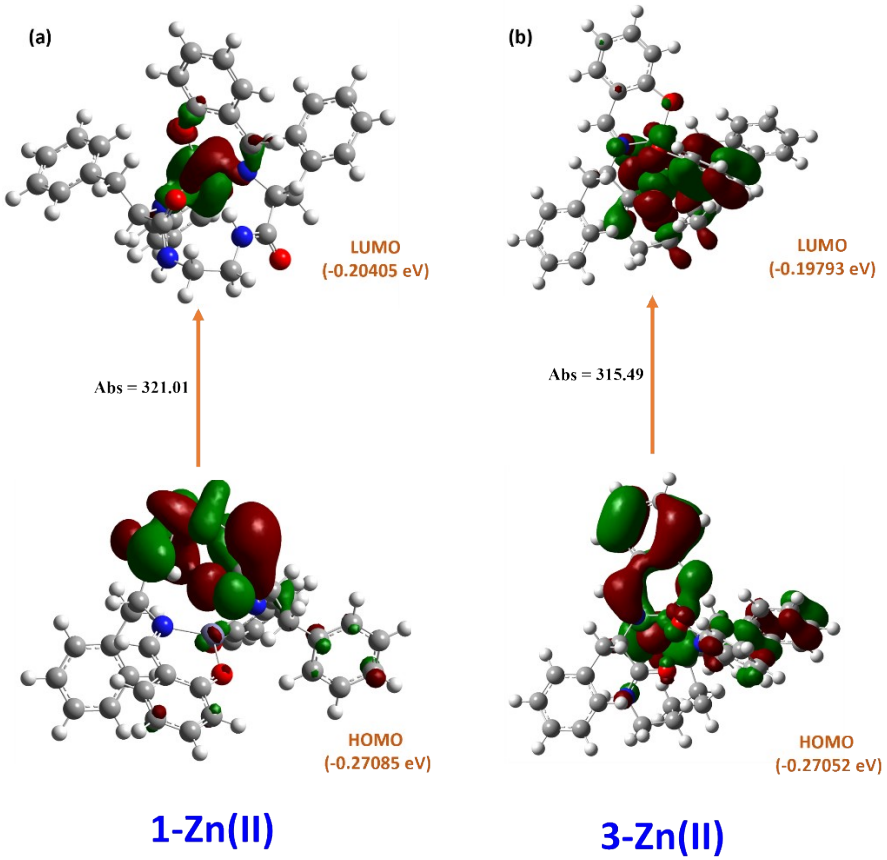

Figure S34. Representation of HOMO-LUMO of **1**-Zn (II) (a) and **3**-Zn (II) (b) complexes by TD-DFT.

Table S1 Quantum yield of neat **1-3** and its complex (**1-3**-Zn(II))

S.No	Entry	Quantum yield
1	**1**	0.31
2	**1**-Zn(II)	0.91
3	**2**	0.24
4	**2**-Zn(II)	0.62
5	**3**	0.20
6	**3**-Zn(II)	0.33

Table S2 Fluorescence decay parameters of neat **1-3** and its complex (**1-3**-Zn(II)) in HEPES buffer (Ethanol:Water = 3:7 v/v, pH ~ 7.4; 10μM; at r.t.)

S.No.	Entry	(A)	τ (ns)	<τ> (ns)
1	**1**	0.73034 (A_1)	0.66225 (τ_1)	
2		0.02759 (A_2)	17.74655 (τ_2)	1.2840
3	**1**-Zn(II)	0.59336 (A_1)	0.70774 (τ_1)	
4		0.16378 (A_2)	8.64393 (τ_2)	1.8356
5	**2**	0.77839 (A_1)	0.67571 (τ_1)	
6		0.12104 (A_2)	0.18469 (τ_2)	0.6095
7	**2**-Zn(II)	0.51118 (A_1)	0.87242 (τ_1)	
8		0.16355 (A_2)	10.55322 (τ_2)	3.2187
9	**3**	0.78198 (A_1)	0.6308 (τ_1)	

10		0.05877 (A_2)	7.12217 (τ_2)	1.0843
11	**3**-Zn(II)	0.67029 (A_1)	0.61534 (τ_1)	
12		0.08508 (A_2)	7.50037 (τ_2)	1.3908

Dynamic parameters determined from $A_1\exp(-x/\tau_1) + A_2\exp(-x/\tau_2) + y_0$

The weighted mean lifetime $<\tau>$ was calculated by using following equation:

$<\tau> = (A_1\tau_1 + A_2\tau_2) / (A_1 + A_2)$

where, A_1/A_2 and τ_1/τ_2 are the fractions (A) and lifetimes (τ) respectively.

Solution concentration = 10 μM.

Table S3 Comparative limit of detection (LOD) of **1-3** with Zn(II) ion.

S.No.	**Sensor**	**Mechanism**	**LOD**	**References**
1	**1** **2** **3**	PET PET PET	8.30×10^{-6} M **or** (8.30 μM) 8.28×10^{-7} M **or** (0.828 μM) 8.34×10^{-7} M **or** (0.834 μM)	**This work**
2	4	-	1.1×10^{-5} M **or** 11 μM	[1]
3	5	-	5.1 μM	[2]
4	6	PET	1.2 μM	[3]
5	7	ratiometric	2.82 μM	[4]
6	8	ICT	1.24 μM, 0.85 μM	[5]
7	9	-	1.2 μM	[6]

Materials and instruments

Z-L-Phenylalanine procured from SRL and N-Hydroxysuccinimide procured from Avra, while salicylaldehyde, DCC, HBr\ Acetic Acid, and all aliphatic spacer including, Ethylene diamine, 1,4 Diaminobutane and Hexamethylenediamine were procured from Sigma-Aldrich,

India. Various metal salts including, $AgNO_3$, $Ca(NO_3)_2 \cdot 4H_2O$, $Cd(NO_3)_2 \cdot 4H_2O$, $Co(NO_3)_2 \cdot 6H_2O$, $Cu(NO_3)_2 \cdot 3H_2O$, $Fe(NO_3)_3 \cdot 9H_2O$, $Hg(NO_3)_2$, KNO_3, $NaNO_3$, $Ni(NO_3)_2 \cdot 6H_2O$, $Pb(NO_3)_2$, and $Zn(NO_3)_2$ were procured from Himedia.

^{1}H-NMR spectra frequency at 500 MHz and ^{13}C-NMR spectra frequency at 126 MHz were performed on a JEOL 500 FT-NMR. Absorption (UV-Visible) spectra were performed on Agilent Cary 60 UV-Visible with serial no.-MY19329220 single beam UV-Visible spectrometer and fluorescence spectra were performed on Fluoromax$^+$ spectrofluorometer at room temperature with a 10 mm quartz cell. While Mass spectra were recorded on SCIEX X500R (QTOF-MS) mass spectrometer. AFM measurements were performed on NT-MDT, with model no. Solver next. Circular Dichroism (CD) spectra were recorded by JASCO J-1500-450 with serial no. D062161638, power A C 220V 50/60HZ 770VA and all spectral data of **1-3** were carried out at room temperature in the range 200-300 nm by using a quartz cuvette (4ml path length, 1cm) and samples were prepared in ethanol with a concentration of 10μM. Dynamic light scattering (DLS) study was performed on Zetasizer Ultra (ZSU5700). Transmission Electron Microscopy (TEM) analysis was recorded on TECNAI 20G2 with 200KV accelerating voltage.

General method for absorption and emission measurement:

Stock solution of **1-3** (10 μM), was prepared in HEPES buffer (Ethanol:Water = 3:7 v/v, pH ~ 7.4; 10μM; at r.t.) for the optical measurement at room temperature with quartz cuvette (4ml, path length, 1cm). Various metal ion (nitrates salt) solutions (100 μM) including, Ag(I), Ca(II), Cd(II), Co(II), Cu(II), Fe(III), Hg(II), K(I), Na(I), Ni(II), Pb(II), and Zn(II) were prepared in doubly-distilled water for metal ion selectivity measurement. In titration measurement, metal ions solution added portion wise in 3.0 ml solution of **1-3** in a quartz cuvette.

Bovine Serum Albumin (BSA) solution preparation

The Bovine Serum Albumin (BSA) stock solution was prepared in HEPES buffer at a pH ~ 7.4. This involved dissolving the appropriate amount of BSA at room temperature and stirring for 1-2 hours. The BSA concentration, determined to be around 19×10^{-6} M (~ 20 μM) was established by using absorption spectroscopy. The calculation involved dividing the absorbance at 280 nm by the molar extinction coefficient of BSA (ε_{280} = 44,300 M^{-1} cm^{-1}).[7,8] The stock solution was stored at 4°C and recommended for use within 4-5 days.

Deconvolution Process:

o Baseline Correction: Ensure accurate peak assignment by removing baseline drift (https://doi.org/10.1111/j.1745-7270.2007.00320.x).

o Smoothing: Reduce noise using smoothing algorithms (https://doi.org/10.1007/978-1-0716-2930-7_15).

o Curve Fitting: Decompose the amide I band into individual component peaks corresponding to different secondary structures (https://doi.org/10.1007/s00249-021-01502-y).

- Peak Assignment: Assign specific peaks to secondary structures based on characteristic absorption frequencies.
- Interpretation of Deconvoluted Spectra

• Peak at 1600-1660 cm^{-1}: The presence of this peak indicates the presence of β-sheet (https://doi.org/10.1039/D0NJ01501F) (https://doi.org/10.1007/s00249-021-01502-y).

• Relative Intensity: The intensity of the β-sheet peak relative to other peaks can provide information about the proportion of β-sheet content (https://doi.org/10.1039/D0NJ01501F) (https://doi.org/10.1007/s00249-021-01502-y).

- A deconvoluted IR spectrum with the amide I band showing several peaks:

• A prominent peak around 1630 cm^{-1} indicating significant β-sheet content.

- Peaks at other wavelengths (e.g., 1660 cm^{-1} and 1670 cm^{-1} for antiparallel β-sheet).

This deconvoluted spectrum can be used to quantify the secondary structure composition of the protein.

Reference

(1) S. Peng, J. Lv, G. Liu, C. Fan, S.Pu, *Tetrahedron* 2020, **76,** 131618.

(2) P. S. Kumar, K. P Elango, *Spectrochim. Acta Part A Mol. Biomol. Spectrosc.* 2020, **241,** 118610.

(3) H.Kim, J. Kang, K. B. Kim, E. J. Song, C.Kim, *Spectrochim. Acta Part A Mol. Biomol. Spectrosc.* 2014, **118,** 883–887.

(4) V. V. S. Mummidivarapu, K. Tabbasum, J. P. Chinta, C. P.Rao, *Dalt. Trans.* 2012, **41**, 1671–1674.

(5) Y. Hu, Y. Liu, G. Kim, E. J. Jun, K. M. K. Swamy, Y. Kim, S.-J. Kim, J. Yoon, *Dye. Pigment.* 2015, **113,** 372–377.

(6) H. Xu, R. Miao, Z. Fang, X.Zhong, *Anal. Chim. Acta* 2011, **687**, 82–88.

(7) A. Ray, B. K. Seth, U. Pal, S. Basu, *Spectrochim. Acta Part A Mol. Biomol. Spectrosc.* 2012, **92**, 164–174.

(8) E. Alarcón, A. Aspée, M. González-Béjar, A. M. Edwards, E. Lissi, J. C.Scaiano, *Photochem. Photobiol. Sci.* 2010, **9**, 861–869.